EFFECT OF TANK SEQUENCING ON CCL ACCELERATORS[†]

C. C. Paulson, R. A. Hartley

Grumman Space Systems Division, 4 Independence Way, Princeton, N.J. 08540

ABSTRACT

For some high energy accelerator applications, coupled cavity structures provide the most efficient means of ion acceleration. This paper describes the results of a beam dynamics study into the effects of the use of various tanking sequence schemes on beam dynamics. The study was performed using two recently developed codes; a central particle pre-processor code and a multi-particle PIC CCL design code "PARMCCL". Particular attention is paid to transverse and longitudinal emittance growth. For a portion of the study, a particle distribution derived from PARMILA was used to prevent a free energy driven (changing of beam distribution) emittance growth. Additionally TRACE-3D has been modified to provide a matched beam for the CCL tanks.

Introduction

This paper presents brief descriptions of a Central Particle pre-processor CCL code (CPCCL) and a Particle-in-Cell (PIC) design code (PARMCCL) that have recently been developed. At present, only Side Coupled CCL structures have been included in these codes. PARMCCL is based on PARMILA and provides a logical extension of the ion accelerator design process.

Linear accelerator tanks are composed of a series of N coupled resonant cavities. Each set of boundary conditions defines N Electric and Magnetic field configurations (modes) which will resonate within the tank. The standard DTL configuration corresponds to the 0 Mode solution in which the Electric fields in all of the cavities are in phase. The synchronous condition for such an in-phase set is that the ions must travel the distance (L) from the center of one cell to the center of the next in one RF period ($L = \beta\lambda$). The π-mode configuration corresponds to a system with a 180° phase change between adjacent cells. In this case, the synchronous condition is $L = \beta\lambda/2$. The standard CCL configuration is the $\pi/2$ mode. In this configuration ion acceleration is obtained from every other cell. (Every other cavity has amplitude ±1, intermediate cavities are empty.) The intermediate (unexcited) cells are termed "coupling cavities" and used for power transfer down the tank. The most common method of designing CCL structures is to remove the coupling cavities from the beamline entirely (for example; Annular, Slot, and Side Coupled CCLs). The cells remaining on the beamline then resemble a $\pi/2$ mode structure and the synchronous condition remains $L = \beta\lambda/2$. Although not a requirement, due to cost considerations, most CCLs are designed with each cell within a tank being identical.

The following two sections describe the multi-particle PIC code PARMCCL and the central particle code CPCCL.

The final sections describe results obtained and items that remain to be done.

Parmccl

The code PARMCCL is broken into two sections: a central particle section that provides the cell table; and a particle dynamics section. The cell tables are calculated in the central particle section and are based entirely on the axial field component. They employ a central particle concept in which the beam is characterized by the parameters of the particle at the bunch center, rather than the more standard synchronous particle concept. The largest effect of this changed viewpoint is found in the phase. Since each cell in a CCL tank is geometrically identical, the phase that the central particle in a bunch sees in the tank varies from cell to cell. Allowing the term "synchronous phase" to refer to a particle having the tank design beta, the relationship between the central phase and the synchronous phase in cell i is given by:

$$\phi_i = \phi_s - \pi(1 - \beta_o/\beta_i).$$

The energy gain in CCL cell i can be written[1]:

$$\delta W_i = \int E_z^{(i)}(r,z,t)\, dz$$

$$= \int \left\{ 2E_oT\, I_o(kr) \cos\left(\frac{2\pi z}{L_2}\right)\right\} \cos(\omega t_i + \phi_i)\, dz \ .$$

In the above equation, the length L_2 refers to $\beta_o\lambda$ ($= 2L_0$) and the variable T refers to the standard Transit Time Factor defined in SUPERFISH. The Modified Bessel Function I_o has been included in the equation since it enters into the determination of the radial Electric field and circumferential Magnetic field for tracking the particles through the CCL. However, all equations are linearized { $I_o(kr) \approx 1$ and $I_1(kr) \approx kr/2$ } in the code.

Defining the ratio of the design beta of the tank and the central beta of the bunch in cell i to be $\beta_i = \beta_o/(1 + \Gamma_i)$ and expanding the functions proportional to the beta ratio, the energy gain equation can be rewritten as:

$$\delta W_i = \int 2 E_oT\, dz\{f_i\cos(\phi)_i - g_i\sin(\phi)_i\} \ ,$$

where: $f_i = \cos^2(x) - \Gamma_i \cdot x \cdot \cos(x) \cdot \sin(x) - \frac{\Gamma_i^2}{2}x^2 \cdot \cos^2(x)$,

$$g_i = \cos(x) \cdot \sin(x) + \Gamma_i \cdot x \cdot \cos^2(x) - \frac{\Gamma_i^2}{2}x^2 \cdot \cos(x) \cdot \sin(x) \ ,$$

and $x = 2\pi z/L_2$.

The cell tables are generated by dividing each cell into two halves, using average values in each cell half for each of the trigonometric terms above, and iterating for a self-consistent

solution to the energy gain equation and the cell phase equation. To allow for examining "as built" configurations in which the set of tank design betas (β_o) is known, it may be input at run time. Alternatively, the code will perform an additional iteration to determine the set, or any combination of the cases may be employed.

In describing the motion of the particles through the CCL, the three field components derived from Maxwell's Equations are used. These are:

$$E_z(r,z,t) = \left\{ 2E_oT \cos\left(\frac{2\pi z}{L_2}\right) \right\} \cos\left(\omega t_i + \phi_i\right)$$

$$E_r(r,z,t) = 2E_oT \frac{\pi r}{2L_0} \sin\left(\frac{2\pi z}{L_2}\right) \cos\left(\omega t_i + \phi_i\right)$$

$$B_\vartheta(r,z,t) = -2E_oT \frac{\omega r}{2c^2} \cos\left(\frac{2\pi z}{L_2}\right) \sin\left(\omega t_i + \phi_i\right)$$

In this portion of the code, each cell is broken into a predetermined (selectable at run time) number of sections, and each particle is followed using the drift - momentum kick - drift method described below. A space charge impulse is applied to each particle at the center of each cell.

For each cell section, all particles are allowed to drift to the center of the section by iterating for the average velocity for each particle in the section. After reaching the center of

the sections, each particle receives a transverse impulse (equal time of flight is used for each particle):

$$\delta P_x^{(i)} = \frac{W_o}{c} \delta(\beta\gamma)_x^{(i)} = \int \overline{F_{(i)}} \cdot dt \cdot \overline{F_{(i)}} \frac{\lambda}{4c}$$

$$\text{with} \qquad \overline{F_x^{(i)}} = \overline{E_x} - \overline{\beta_i cB_\vartheta}.$$

The average radial Electric field and circumferential Magnetic fields are found in the same manner as the average axial field

$$\overline{E_r} = A \frac{\pi r}{2 \cdot L_0} \left\{ \overline{T^{(i)}} \cdot \cos \vartheta_i - \overline{S^{(i)}} \cdot \sin \vartheta_i \right\} \qquad \text{and}$$

$$\overline{B_\vartheta} = A \frac{\beta_0}{c} \frac{\pi \cdot r}{2 \cdot L_0} \left\{ \overline{V^{(i)}} \cdot \cos \vartheta_i - \overline{U^{(i)}} \cdot \sin \vartheta_i \right\} .$$

The sequence followed by the particles in traversing a cell with N sections (N must be even) is therefore given by :

$$[DMD]_1 \ [DMD]_2 \ \cdots \ [DMD]_{N/2} \ [SC]$$
$$[DMD]_{N/2+1} \ [DMD]_{N/2+2} \ \cdots \ [DMD]_N$$

In this relation, $[DMD]_i$ refers to Drift-Momentum kick-Drift sequence described above, and [SC] refers to the Space Charge momentum kick. In this code an equal "time of flight" concept is employed rather than that of "equal distance traveled". The space charge calculator has been rewritten to reflect this. Additionally, the routine has been rewritten to transform all particle coordinates to the particles' frame of reference prior to performing its calculations, to avoid any possible relativistic problems.
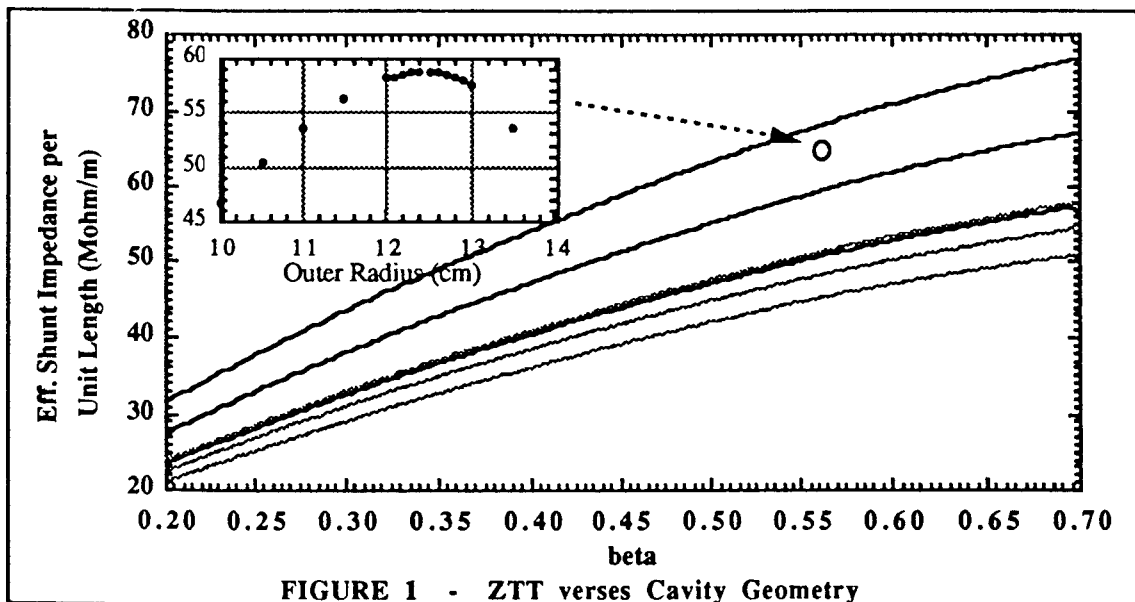

FIGURE 1 - ZTT verses Cavity Geometry

Central Particle Code

The major limitation of multi-particle PIC simulation codes is the time required to run them. Using a PIC code for trade studies is an arduous time-consuming process. In all types of accelerators, beam dynamics design requires the determination of many interacting parameters. CCLs have a

particular problem - - a "best" design technique has not been prescribed to date. Providing the examination of the CCL parameter space to determine acceptable compromises between parameters almost necessitates the use of a preprocessor code.

In the present instance, this ability to rapidly scan the CCL operating space to determine parameter values is being

provided by the code CPCCL. In this code, the energy gain in each cell is given by:

$$\delta W_i = \frac{E_o T L_o}{2}\left(1 - \frac{\Gamma_i}{2}(1 + 0.322467 \cdot \Gamma_i)\right) \cos \phi_i \quad,$$

with the cell phase and cell beta ratio (Γ_i) given by the same equations as in section 2. Since the accuracy found in PARMCCL is not required in this instance, the cell central beta is defined to be:

$$\beta_i = \beta\left(W + \frac{\delta W}{2}\right) \quad.$$

As before, self-consistent iterations are used to determine the tank and cell tables. Some of the inputs required for this code are:

E_o : Average accelerating field, **or**
σ_{Lo} : zero current longitudinal phase advance,
B' : Magnetic Field Gradient, **or**
σ_{To} : zero current transverse phase advance,
r_b : bore radius,
R : Cell outer radius,
I : Current,
f : frequency,
W_{in} : Input Energy,
W_{out} : Input Energy,
A : particle species,
φ : phase (absolute value),
N,M : no. of cells per tank, and cell lengths per magnet.

Items such as the shunt impedance, transit time factor, maximum surface field, quality, and gap length (along with the quantities derived from them such as the power consumed) are obtained from scaling from curves. These curves have been generated using data obtained from multiple SUPERFISH runs, and from references 2, 3 and 4. Additional quantities such as the current limit are obtained in the standard manner[5].

Figure 1 shows the Shunt Impedance per unit length as a function of beta, frequency, bore radius, and outer radius. The three solid curves are for an outer radius (R) of 12.6 cm, a frequency of 850MHz, and bore radii (r_b) of 0.5, 1.0 and 1.5 cm. The three dashed curves are for the same radii (R and r_b) at a frequency of 425MHz. (The two cases [f=425 MHz, r_b=0.5 cm] and [f=850 MHz, r_b=1.5 cm] lie on top of one another.) The insert shows the effect of the cavity outer radius.

Results

To provide a test of the code a series of runs were made to look at the effect of tank sequencing on the beam dynamics. Similar tanks were generated by varying the number of cells in the tank, the Magnetic focussing strength, and the accelerating field strength. For these tanks similarity was defined as maintaining the transverse focussing strength per unit length and accelerating field per unit length constant. In each tank, the transverse focussing element was a single (constant length) PMQ that was centered in a length $\beta_o \lambda /2$. The initial CCL used was one in which each tank consisted of one cell and a PMQ. For the one-cell tank, the values chosen were:

$$B' = (B')_1 = 50 \text{ Ts/m} \quad \text{and}$$
$$E_o T = (E_o T)_1 = 7.5 \text{ MV/m}.$$

The parameters for the other tanks are then given by:

$$(B')_n = \{(n+1)/2\}(B')_1 \quad \text{and}$$
$$(E_o T)_n = \{(n+1)/2n\}(E_o T)_1 \quad.$$

TRACE-3D was used to determine the matched beams for each case considered. Table 1 lists the phase advances found for the zero current and full current (100mA) cases for each configuration where a matched beam could be determined. Although the configurations were designed to be similar, they can be seen to cover a reasonably wide operational range.
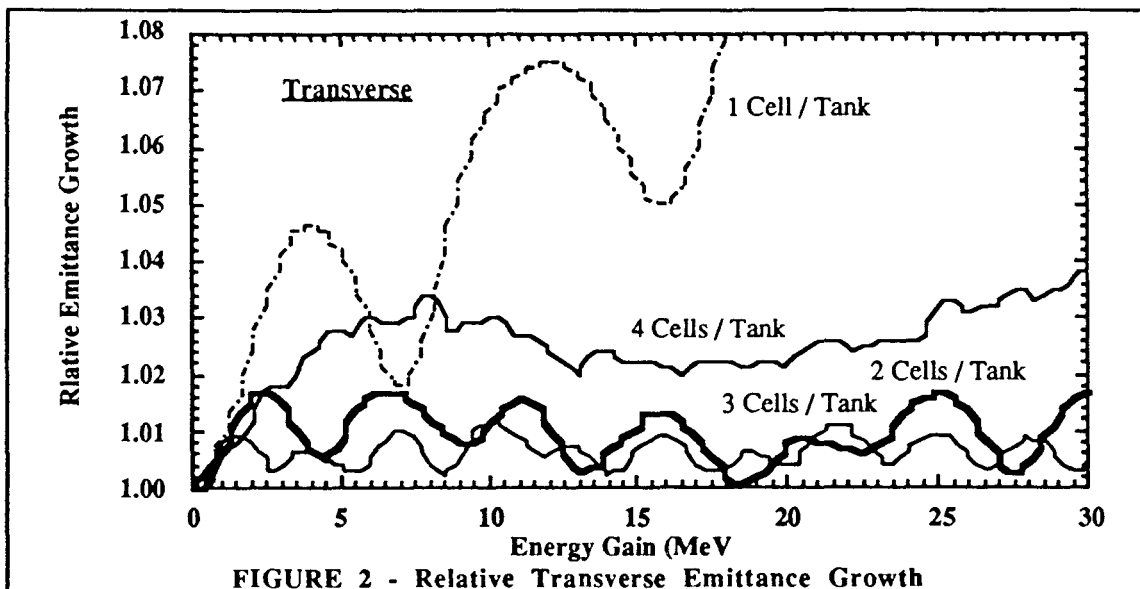

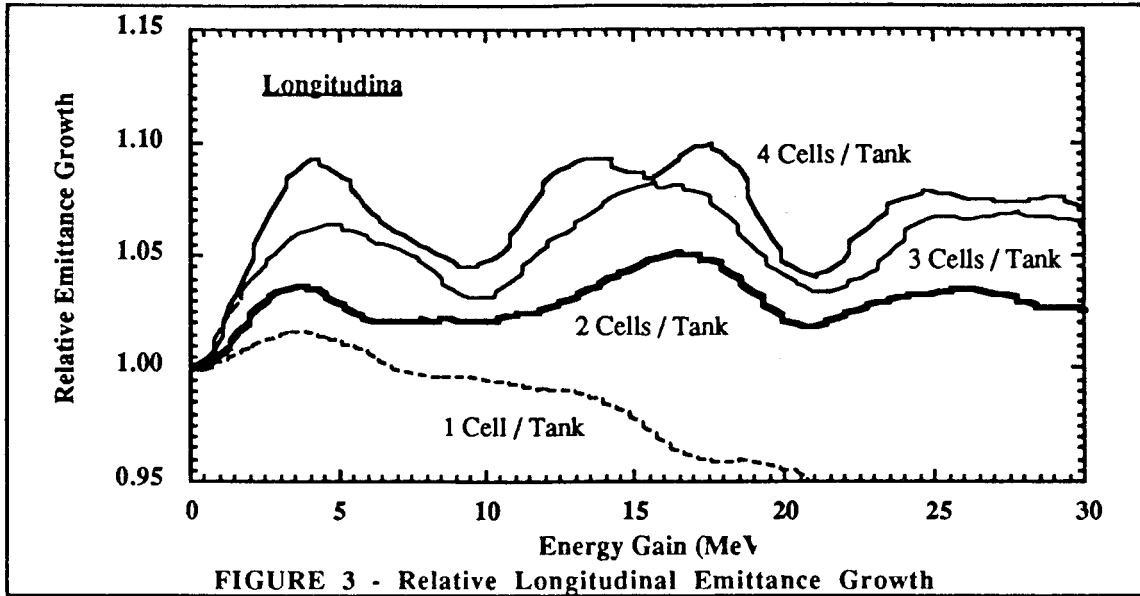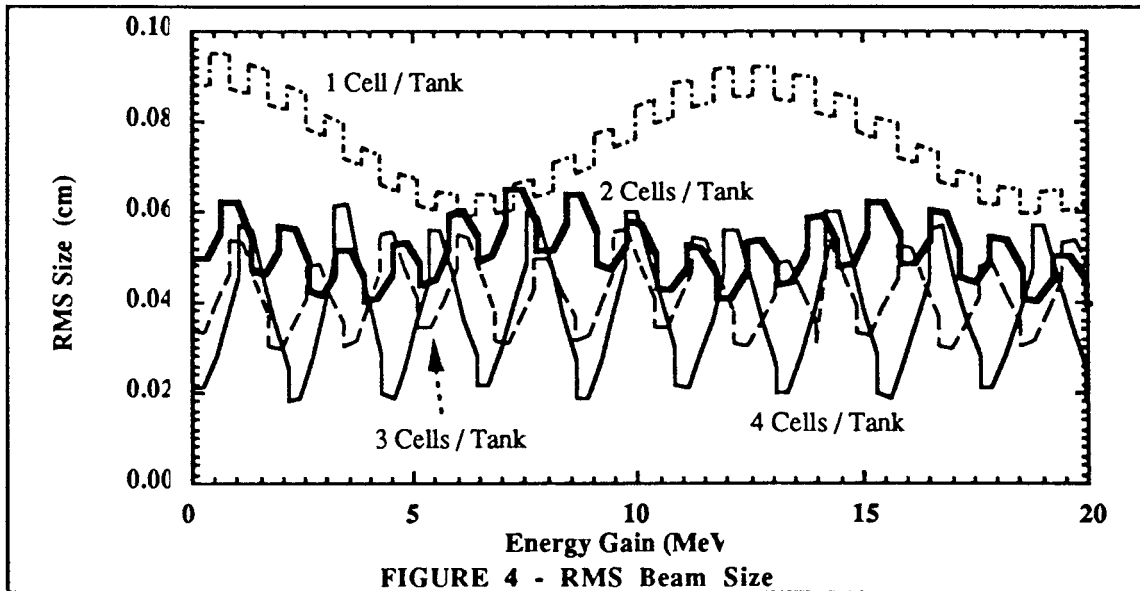FIGURE 2 - Relative Transverse Emittance Growth

FIGURE 3 - Relative Longitudinal Emittance Growth

TABLE 1 - Phase Advances (per tank length)

Configuration	σ_{T_0} (deg)	σ_{L_0} (deg)	σ_T (deg)	σ_L (deg)
1 Cell / Tank	12.8	10.3	4.5	5.3
2 Cells/Tank	34.6	15.4	18.0	6.0
3 Cells/Tank	68.2	20.5	43.5	6.9
4 Cells/Tank	(no match found)		93.1	7.9
5 Cells/Tank	(no match found)		(no match found)	

FIGURE 4 - RMS Beam Size

Figures 2 and 3 show the relative Transverse and Longitudinal emittance growths over a 30 MeV energy range for the full current cases. It can clearly be seen that case 1 corresponds to an under-focussed system and case 4 to an over-focussed system. In case 4, it is the space charge that is maintaining the stability of the system. Cases 2 and 3 are

relatively stable. Figure 4 shows the beam radius for the four cases. The relatively flat sections are the magnet locations.

Conclusions

A set of codes has been presented to help design CCL accelerators. The two codes are complementary in method and result type. The central particle code CPCCL allows the designer to rapidly scan the operating space to obtain acceptable compromises between design parameters. The PIC code PARMCCL provides a much more accurate assessment of the operating characteristics of a side coupled CCL. However, it requires relatively long run times.

The designer has available two variables to alter the run time of PARMCCL. These are the number of macro particles used and the number of sections in which to divide each cell. The code is presently running on two different computers: a μ-Vax, and an Stardent Titan (3 CPUs). On the μ-Vax, the code requires approximately 2 hours to calculate results over a 100 MeV range using two sections per cell in a 1000 particle simulation. Using eight sections per cell, this increases to approximately 5 hours. On the Titan, the two section per cell case runs in approximately 30 minutes and the eight section per cell to a little over 2 hours. To date, no attempt was made to make the code vectorizable.

A preliminary assessment has been made of the effect of number of cell section on emittance values. Eleven runs were made using 2 sections per cell and 12 runs were made using eight sections per cell. Each run was made using a different seed for the initial distribution random number generator. The mean transverse emittance and the standard deviation of the transverse emittance results for the the different cases were identical. The results for the longitudinal emittance differed slightly with the means differing by 0.4% and the standard deviations by ~3% (of a very small number). Since this evaluation was completed, most runs have used two sections per cell.

A second major limitation of the code, at present, is its restriction to a particular type of CCL. Work will be ongoing to expand this capability.

Acknowledgement

References

1. K. R. Crandall; "TRACE-3D Documentation", LA-11054-MS, pages 74-81, Los Alamos National Laboratory, Los Alamos NM, August 1987.

2. J. J. Manca, E. A. Knapp; "TM_{01} Mode Accelerating Cavity Optimization", LA-7323, Los Alamos National Laboratory, Los Alamos NM, August 1978.

3. Dr. R. W. Hamm (Princ. Investigator); "Final Technical Report - Space-Based Neutral Particle Beam Linear Accelerator Scaling Study", AccSys Technology, Inc., Pleasanton Ca., September 1987.

4. "FERMILAB LINAC Upgrade - Conceptual Design", Fermi National Accelerator Laboratory, Batavia Ill, November 1989.

5. T. P. Wangler; "Space-Charge Limits in Linear Accelerators", LA-8388, UC-28, Los Alamos National Laboratory, Los Alamos NM, December 1980.